Available online at www.sciencedirect.com
ScienceDirect
Trans. Nonferrous Met. Soc. China 24(2014) 4023−4029
Transactions of Nonferrous Metals Society of China
www.tnmsc.cn

Effect of sintering temperature on cycling performance and rate performance of $LiNi_{0.8}Co_{0.1}Mn_{0.1}O_2$

Xiang-qun LI[1], Xun-hui XIONG[2], Zhi-xing WANG[2], Qi-yuan CHEN[1]

1. School of Chemistry and Chemical Engineering, Changsha 410083, China;
2. School of Metallurgy and Environment, Central South University, Changsha 410083, China

Received 8 January 2014; accepted 20 October 2014

Abstract: $LiNi_{0.8}Co_{0.1}Mn_{0.1}O_2$ powder was prepared by mixing $LiOH·H_2O$ and co-precipitated $Ni_{0.8}Co_{0.1}Mn_{0.1}(OH)_2$ at a molar ratio of 1:1.05, followed by sintering at different temperatures. The effects of temperature on the morphology, structure and electrochemical performance were extensively studied. SEM and XRD results demonstrate that the sintering temperature has large influence on the morphology and structure and suitable temperature is very important to obtain spherical materials and suppresses the ionic distribution. The charge−discharge tests show that the electrochemical performance of $LiNi_{0.8}Co_{0.1}Mn_{0.1}O_2$ powders becomes better with the increase of temperature from 700 °C to 750 °C and higher temperature will deteriorate the performance. Although both of materials obtained at 750 °C and 780 °C demonstrate almost identical cyclic stability at 2*C* rate, which delivers 71.9% retention after 200 cycles, the rate performance of powder calcined at 780 °C is much poorer than that at 750 °C. The XRD results demonstrate that the poor performance is ascribed to more severe ionic distribution caused by higher temperature.
Key words: lithium ion battery; $LiNi_{0.8}Co_{0.1}Mn_{0.1}O_2$; sintering temperature; cycling performance; rate performance

1 Introduction

Due to the advantages including high operation voltage, high energy density, long cycle life, light mass, small volume, low self-discharge rate, non-memory effect and environment-friendly, lithium ion batteries are considered the most attractive choice among rechargeable batteries. During the past decades, lithium ion batteries have been widely used in the small electronic devices, including cell phones, laptop computers and video cameras [1,2]. $LiCoO_2$ layered cathode material has been extensively used as a promising candidate for commercial applications. However, its further development is limited by the toxicity and high expense of cobalt [3]. Due to the Jahn−Teller effect, $LiMn_2O_4$ suffers from the problems such as the fast decrease of electric capacity and the poor cycling performance [4,5]. Similar with $LiCoO_2$, $LiNiO_2$ also exhibits layered structures. In spite of the low-cost, low toxicity and large electric capacity, the serious cation mixing Li^+/Ni^{2+} has remarkable influence on the electrochemical performance of lithium ion batteries. Besides, the safety problem of $LiNiO_2$ still needs to overcome [6,7]. The cathode material $LiNi_{1-x-y}Co_xMn_yO_2$ with layed structure not only inherits its good cycling performance of $LiCoO_2$, high specific electric capacity of $LiNiO_2$ and thermal stability of $LiMn_2O_4$, but also shows low-toxicity and low-cost [8]. Owing to its high specific capacity (>200 mA·h/g) and good cycling stability, $LiNi_{0.8}Co_{0.1}Mn_{0.1}O_2$ possesses a great potential to replace $LiCoO_2$ as the cathode material of high-capacity batteries used in electric vehicles and hybrid electric vehicles. Thus, it has attracted increasing attention in recent years [9,10].

In order to improve the electrochemical properties of Ni-rich materials, the parameters of the synthesis process have been extensively investigated. CHEN et al [11] found that the spherical $Ni_{0.8}Co_{0.1}Mn_{0.1}(OH)_2$ precursor with average size about 0.5 μm could be prepared by controlling the speed of co-precipitation, and the obtained $LiNi_{0.8}Co_{0.1}Mn_{0.1}O_2$ showed excellent cycling performance. HU et al [12] evaluated the effect of stirring speed, pH value, concentration of ammonia and reaction time in co-precipitation process on the morphology, size distribution and tap density of the

Foundation item: Project (2014CB643406) supported by the National Basic Research Program of China
Corresponding author: Zhi-xing WANG; Tel: +86-731-88836633; E-mail: zxwang21@16.3com
DOI: 10.1016/S1003-6326(14)63564-0

$Ni_{0.8}Co_{0.2}(OH)_2$ precursor. Besides, the effects of sintering parameters on the electrochemical performance of $Ni_{0.8}Co_{0.2}(OH)_2$ were investigated in the optimum precursor fabrication process. ZHONG et al [13] prepared $Ni_{0.8}Co_{0.2}(OH)_2$ with metal nitrate using maleic acid and ethanol as solution and the specific capacitance showed an increasing tendency instead of decreasing after 25 cycles. LI et al [14] produced $LiNi_{0.8}Co_{0.1}Mn_{0.1}O_2$ via the rapid coprecipitation technique with metal chloride. The results showed that the materials fabricated by rapid coprecipitation exhibited low cation mixing and good electrochemical properties.

Sintering temperature and sintering time are the most important parameters for both conventional high temperature solid-state reaction and wet chemical pre-treated solid-state reactions including sol−gel and coprecipitation method. The migration of Li^+ and the active energy needed for lattice reconstruction determine that the reaction must happen at a certain temperature. The distance between ions and the complexity of the lattice determine that the reaction should completely finish at a certain period. Accordingly, in the present work, the effects of sintering temperature on the morphology, microstructure and electrochemical performance, especially rate performance of $LiNi_{0.8}Co_{0.1}Mn_{0.1}O_2$ were investigated.

2 Experimental

2.1 Sample preparation

$LiOH·H_2O$ (excess coefficient=1.05) and $Ni_{0.8}Co_{0.1}Mn_{0.1}(OH)_2$ were weighed according to the stoichiometric ratio, followed by mixing and grinding in a mortar for 40 min in order to obtain a homogeneous mixture. The mixture was then sintered in a tube furnace under oxygen flow at 700, 725, 750 and 800 °C for 15 h, respectively. After cooling down to room temperature, $LiNi_{0.8}Co_{0.1}Mn_{0.1}O_2$ was fabricated.

2.2 Physical characterization

The phases of the samples were characterized by X-ray diffraction (XRD), which was conducted on a Rigaku diffractometer (Rigaku Corporation, Japan) at 40 kV and 50 mA. The step width, scanning speed and the scanning range of diffraction angle were 0.02°, 10 (°)/min and 10°−85°, respectively. A scanning electron microscope (SEM) (JSM−5600LV, JEOL) was used for microstructural examination.

2.3 Fabrication of battery and electrochemical property tests

Electrochemical charge−discharge tests were performed using the cathode with a mixture of 80% cathode material, 10% super P carbon black and 10% polyvinylidene fluoride (PVDF). The electrolyte was 1.0 mol/L $LiPF_6$/EC+DMC+EMC (1:1:1, volume ratio). Preliminary cell tests were done using 2025 coin-type cell adopting Li metal as an anode with a voltage window of 2.8−4.3 V (versus Li/Li^+) at room temperature. The Neware BTS−5 V/10 mA battery testing system was applied to the charge−discharge cycling tests at different rates. The voltage range was 2.8−4.3 V. The AC impedance experiments were conducted on the US CHI660 electrochemical workstation with the testing frequency ranging from 0.01 Hz to 100 kHz.

3 Results and discussion

3.1 DSC−TG analyses

In order to determine the sintering parameters of $LiNi_{0.8}Co_{0.1}Mn_{0.1}O_2$, the homogeneous mixture of $Ni_{0.8}Co_{0.1}Mn_{0.1}(OH)_2$ precursor and $LiOH·H_2O$ was analyzed by DSC−TG technique as shown in Fig. 1. It is obvious that the reaction consists of four steps. First, from room temperature to 280 °C, the absorbed water and crystal water lost, accompanied by huge heat-absorption and apparent mass loss. The physically absorbed water evaporated from room temperature to 100 °C. The next step was between 100 °C and 230 °C, which is ascribed to the crystal water. The third step was the decomposition of the $Ni_{0.8}Co_{0.1}Mn_{0.1}(OH)_2$ precursor and the melting of LiOH, and following process was the crystallization of $LiNi_{0.8}Co_{0.1}Mn_{0.1}O_2$. After reaching 820 °C, a slight but continuous mass loss was observed, probably due to the decomposition of the crystals. It has been reported that the over-heated sintering leads to the formation of nonstoichiometric $Li_{1-x}MO_{2-y}$ accompanied by precipitation of O and Li [15,16]. Therefore, in order to make sure of the full reaction, the sintering temperature should be controlled in the range of 600−820 °C. Besides, during the sintering process, the

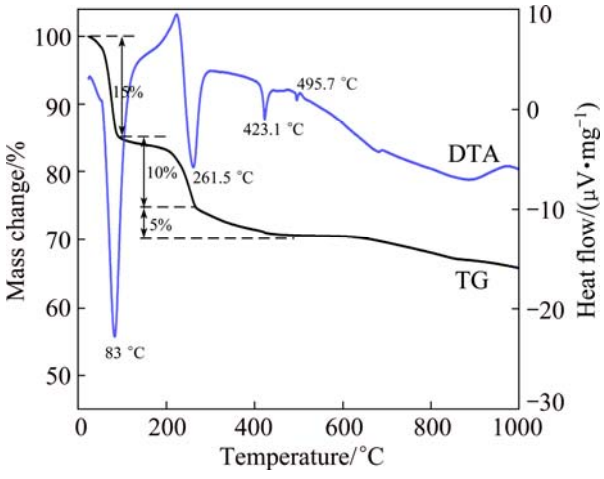

Fig. 1 DSC−TG curves for precursors

samples should be kept around 500 °C for a while, so that the melted LiOH can completely permeate into $Ni_{0.8}Co_{0.1}Mn_{0.1}(OH)_2$.

3.2 Morphology and microstructure analyses

Figure 2 shows the SEM images of the $Ni_{0.8}Co_{0.1}Mn_{0.1}(OH)_2$ precursor and the $LiNi_{0.8}Co_{0.1}Mn_{0.1}O_2$ sintered at different temperatures. Figures 2(a) and (b) show that the precursor samples are spherical with the diameter of 10−12 μm, formed by the agglomeration of tiny rod-like particles. During sintering at 700−750 °C, the precursors are still in regular spheres with the diameter of 10−12 μm with clear boundaries, and the agglomeration is still not apparent. From 700 to 750 °C, the primary particles tend to grow, leading to higher porosity. However, when reaching 780 °C, the primary particles grow significantly, resulting in an obvious morphology change. For the sake of the good mobility for better processability of the electrode fabrication and the high energy density of the lithium ion battery provided by the high tap density of spherical particles, the sintering temperature should be below 780 °C.

Figure 3 shows the XRD patterns of $LiNi_{0.8}Co_{0.1}Mn_{0.1}O_2$ sintered at different temperatures. It is obvious that all samples synthesized at different temperatures exhibit the same α-$NaFeO_2$ structure, in which Li and transition metals occupied 3*a* and 3*b* positions, respectively. There are no impurity peaks in the XRD patterns. The *c*/*a* of the structure is relevant to the stability of the layered structure and when *c*/*a*>4.899, which means that the crystallization of the material is high. The $I_{(003)}/I_{(104)}$ demonstrates the cation disorder of Li and Ni, namely higher $I_{(003)}/I_{(104)}$ and lower cation disorder [17,18]. Table 1 lists the lattice parameters and $I_{(003)}/I_{(104)}$ values of the $LiNi_{0.8}Co_{0.1}Mn_{0.1}O_2$ calculated by the software Jade. It is clear that the diffraction peak

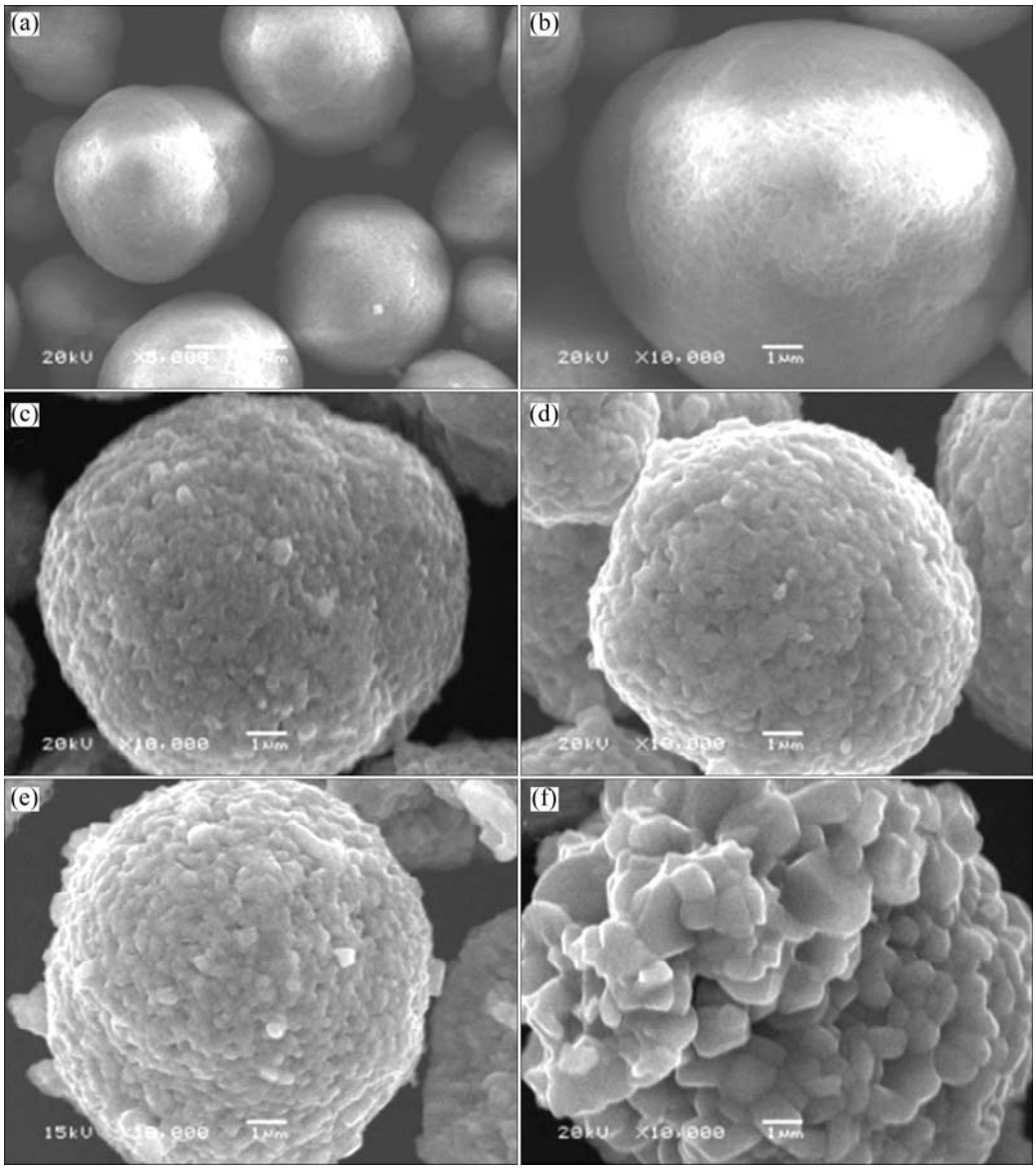

Fig. 2 Typical SEM images of $Ni_{0.8}Co_{0.1}Mn_{0.1}(OH)_2$ precursor (a, b) and $LiNi_{0.8}Co_{0.1}Mn_{0.1}O_2$ sintered at 700 °C (c), 725 °C (d), 750 °C (e) and 780 °C (f)

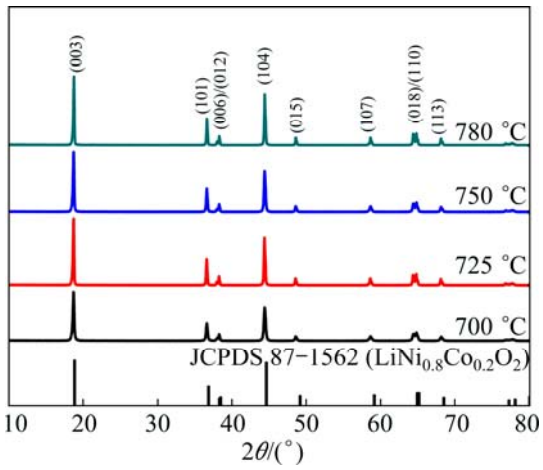

Fig. 3 XRD patterns of $LiNi_{0.8}Co_{0.1}Mn_{0.1}O_2$ sintered at different temperatures

Table 1 Lattice parameters of $LiNi_{0.8}Co_{0.1}Mn_{0.1}O_2$ calcined at different temperatures

Sintering temperature/°C	a/Å	c/Å	V/Å^3	c/a	$I_{(003)}/I_{(104)}$
700	2.8733	14.2051	101.57	4.9438	1.43
725	2.8745	14.2142	101.87	4.9449	1.44
750	2.8749	14.2181	101.76	4.9456	1.48
780	2.8741	14.2052	101.58	4.9425	1.46

intensity and lattice parameter are strongly dependant on the temperature. From 700 °C to 750 °C, c/a increases. This is because with increasing temperature, the formed layer structures tend to be perfect. Besides, higher temperature leads to higher crystallinity, lower lattice stress and larger grain size. Due to the close diameter of Li^+ and Ni^{2+}, they can be easily mixed during sintering. With increasing temperature, the $I_{(003)}/I_{(104)}$ decreases, which is attributed to higher temperature leading to the oxidation of Ni^{2+} to Ni^{3+} and decrease of cation disorder. However, when the temperature is too high, the cation disorder exhibits a further increase. According to the thermodynamic property, Ni^{3+} tends to transform into Ni^{2+} at a much higher temperature. Furthermore, based on the kinetic rate equation, the evaporation speed of Li is proportional to the exponent of the sintering temperature. The accelerated evaporation of Li results in more significant inhomogeneity. As a consequence, it is necessary to further investigate the influence of sintering temperature on the structure of material [9].

Figure 4 shows the initial charge−discharge curves and the cycling performance at 2C for $LiNi_{0.8}Co_{0.1}Mn_{0.1}O_2$ calcined at different temperatures. When the temperature increases from 700 °C to 750 °C, the initial discharging specific capacity increases and the cycling property is improved. The materials calcined at

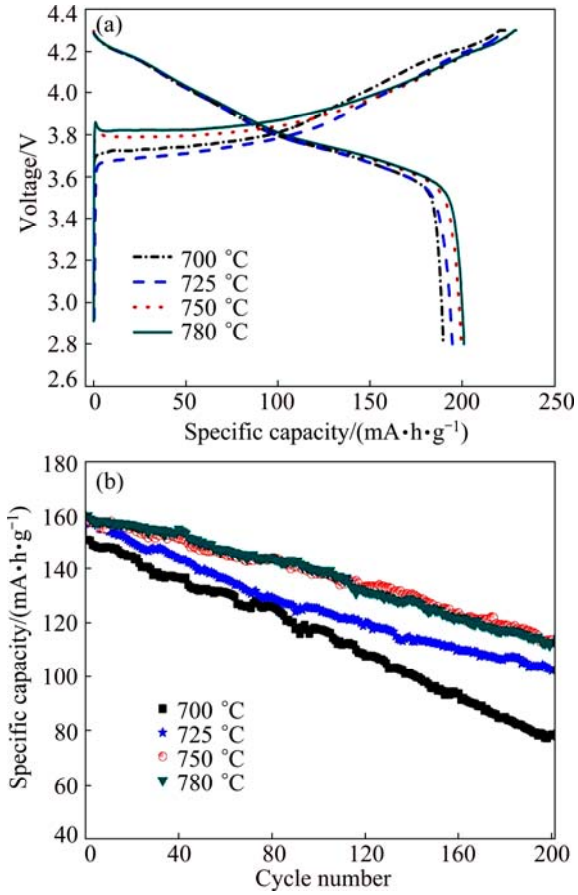

Fig. 4 Initial charging−discharging curves (a) and cycling performance at 2C (b) for $LiNi_{0.8}Co_{0.1}Mn_{0.1}O_2$ calcined at different temperatures

750 °C possess higher initial discharging specific capacity (195.4 mA·h/g), and the capacity after 200 cycles at 2C is 113.7 mA·h/g with a retention of 71.9%. The XRD patterns reveal that the sample calcined at 750 °C exhibits good crystallinity and low cation disorder, leading to the best electrochemical property. However, the initial discharging performance and the cycling properties at 750 °C and 780 °C with 2C were similar, which is not in accordance with the XRD and SEM results. Thus, the reason needs further investigation.

Figure 5 presents the first discharge curves at different rates and rate capability of electrodes as a function of rate after 5 cycles. Due to the low sintering temperatures, the samples sintered at 700 °C and 725 °C exhibit incomplete crystals, large amount of residue Ni^{2+}, severe inhomogeneity and poor rate capability. The results are in accordance with the XRD and cycling performance results. The materials calcined at 750 °C and 780 °C show almost the same performance at the rate lower than 5C. But the capacity of the latter material is far below the former one when charging−discharging at the rate between 5C and 10C. Such a result should be attributed to the transformation of Ni^{3+} into Ni^{2+} and

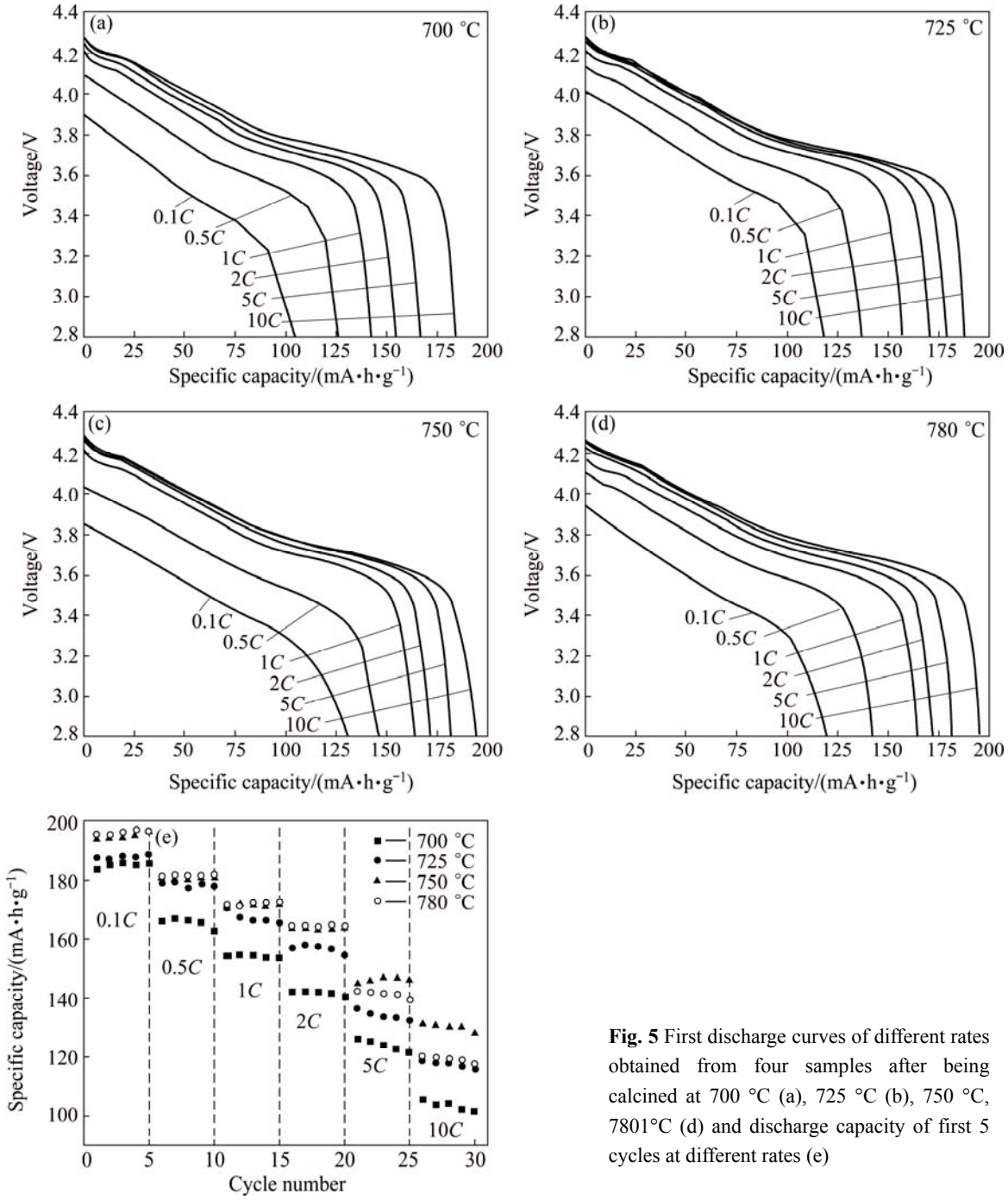

Fig. 5 First discharge curves of different rates obtained from four samples after being calcined at 700 °C (a), 725 °C (b), 750 °C, 7801°C (d) and discharge capacity of first 5 cycles at different rates (e)

higher evaporation speed of Li salt, which will lead more Ni^{2+} to 3*a* position [20,21]. At low current, Ni^{2+} at 3*a* position does not have significant influence on the specific capacity and cycling performance. However, when charging−discharging at a high rate, it inhibits the diffusion of Li^+, resulting in lower rate capability. Figure 5 reveals that the sample calcined at 750 °C shows the best rate capability. The capability at 10*C* is 131.3 mA·h/g, 67.4 % of that at 0.1*C*.

In order to better understand the influence of the two temperatures of 750 °C and 780 °C on the electrochemical performance, XRD was used to characterize the materials sintered at the two temperatures with the scanning angle of 10°−120° and scanning speed of 2 (°)/min. Rietveld method (using the software Fullprof) was applied for the data refinement. Pseudo−Voigt function was used to simulate the diffraction peaks and over 30 parameters including the atomic position, atom occupancies, lattice parameter and isotropic thermal parameters were refined. Figure 6 presents the XRD patterns and Rietveld refinements of $LiNi_{0.8}Co_{0.1}Mn_{0.1}O_2$ obtained at 750 °C and 780 °C. As

shown in Fig. 6, the neglectable difference between experimental data and fitted results indicates that the refined results were reliable. The refinement results indicate that the ratios of cation mixing of the materials processed at 750 °C and 780 °C are 1.6 % and 2.3 %, respectively. Higher cation disorder means more Ni^{2+} at 3*a* position, leading to the restrained diffusion of Li ion at 3*a* position. Thus, the material sintered at 780 °C shows poor electrochemical property, especially at high rates. The results are consistent with the data in Table 2.

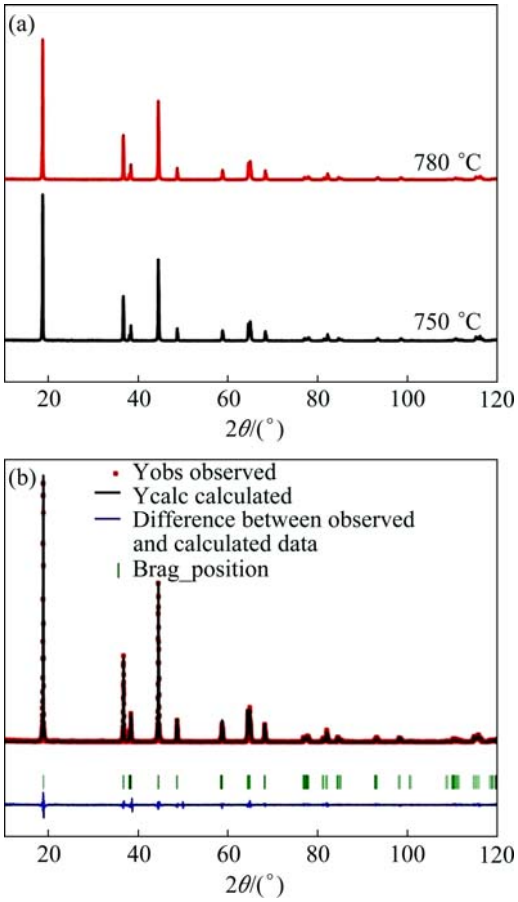

Fig. 6 XRD patterns (a) and Rietveld refinements (b) of $LiNi_{0.8}Co_{0.1}Mn_{0.1}O_2$ obtained at 750 °C and 780 °C

4 Conclusions

1) The influence of sintering temperature on the morphology, structure and electrochemical performance is significant. A proper sintering temperature can not only keep the morphology of spherical particles, but also inhibit the inhomogeneity of Li^+ ions and Ni^+ ions. The $LiNi_{0.8}Co_{0.1}Mn_{0.1}O_2$ sintered at 750 °C shows the best electrochemical performance.

2) $LiNi_{0.8}Co_{0.1}Mn_{0.1}O_2$ sintered at 750 °C shows good cycling performance and rate capability. Its capacity retention ratio is 71.9 % after charging−discharging 200 times at 2*C*. Its capability at 10*C* is 131.3 mA·h/g, which is about 67.4 % of that at 0.1*C*.

References

[1] FERGUS J W. Recent developments in cathode materials for lithium ion batteries [J]. Journal of Power Sources, 2010, 195(4): 939−954.

[2] SCROSATI B. Recent advances in lithium ion battery materials [J]. Electrochimica Acta, 2000, 45(15−16): 2461−2466.

[3] LUO Wen-bin, ZHOU Fu, ZHAO Xue-mei, LU Zhong-hua, LI Xin-hai, DAHN J R. Synthesis, characterization and thermal stability of $LiNi_{1/3}Mn_{1/3}Co_{1/3-z}Mg_zO_2$, $LiNi_{1/3-z}Mn_{1/3}Co_{1/3}Mg_zO_2$ and $LiNi_{1/3}Mn_{1/3-z}Co_{1/3}Mg_zO_2$ [J]. Chemistry Materials, 2010, 22: 1164−1172.

[4] BLYR A, SIGALA C, AMATUCCI G, GUYOMARD D, CHABRE Y, TARASCON J M. Self-discharge of $LiMn_2O_4$/C Li-ion cells in their discharged state: Uderstanding by means of three-electrode measurements [J]. Journal of the Electrochemical Society, 1998, 145(1): 194−209.

[5] AOSHIMA T, OKAHARA K, KIYOHARA C, SHIZUKA K. Mechanisms of manganese spinels dissolution and capacity fade at high temperature [J]. Journal of Power Sources, 2001, 97−98: 377−380.

[6] DAHN J R, SACKEN U, MICHAL C A, Structure and electrochemistry of $Li_{1\pm y}NiO_2$ and a new Li_2NiO_2 phase with the $Ni(OH)_2$ structure [J]. Solid State Ionics, 1990, 44(1−2): 87−97.

[7] DAHN J R, SACKEN U V, JUZKOW M W, AL-JANABY H, Rechargeable $LiNiO_2$/carbon cells [J]. Journal of the Electrochemical Society, 1991, 138(8): 2207−2211

[8] KIM M H, SHIN H S, SHIN D, SUN Y K. Synthesis and electrochemical properties of $Li[Ni_{0.8}Co_{0.1}Mn_{0.1}]O_2$ and $Li[Ni_{0.8}Co_{0.2}]O_2$ via co-precipitation [J]. Journal of Power Sources, 2006, 159: 1328−1333.

[9] SHIM J, KOSTECKI R, RICHARDSON T, SONG X, STRIEBEL K A. Electrochemical analysis for cycle performance and capacity fading of a lithium-ion battery cycled at elevated temperature [J]. Journal of Power Sources, 2002, 112: 222−230.

[10] XIONG Xun-hui, WANG Zhi-xing, GUO Hua-jun, ZHANG Qian, LI Xin-hai, Enhanced electrochemical properties of lithium-reactive V_2O_5 coated on the $LiNi_{0.8}Co_{0.1}Mn_{0.1}O_2$ cathode material for lithium ion batteries at 60 °C [J]. Journal of Materials Chemistry A, 2013, 1: 1284−1288.

[11] CHEN Wei, LI Xin-hai, WANG Zhi-xing, GUO Hua-jun, YUE Peng, LI Ling-jun. Influence of feeding rate on performance of $LiNi_{0.8}Co_{0.1}Mn_{0.1}O_2$ cathode materials [J]. The Chinese Journal of Nonferrous Metals, 2012, 22(7): 1956−1962. (in Chinese)

[12] HU Guo-rong, LIU Yan-jun, PENG Zhong-dong, DU Ke, GAO Xu-guang. Synthesize and properties of spherical cathode materials $LiNi_{0.8}Co_{0.2}O_2$ by controlled crystallization method [J]. The Chinese Journal of Nonferrous Metals, 2007, 17(1): 59−67. (in Chinese)

[13] ZHONG Y D, ZHAO X B, CAO G S, TU T P, ZHU T J. Characterization of particulate sol−gel synthesis of $LiNi_{0.8}C0_{0.2}O_2$ via maleic acid assistance with different solvents [J]. Journal of Alloys and Compounds, 2006, 420(1): 298−305.

[14] LI Ling-jun, LI Xin-hai, WANG Zhi-xing, GUO Hua-jun, YUE Peng, CHEN Wei, WU Ling. A simple and effective method to synthesize layered $LiNi_{0.8}Co_{0.1}Mn_{0.1}O_2$ cathode materials for lithium ion battery [J]. Powder Technology, 2004, 206: 353−357.

[15] HWANG B J, SANTHANAM R, CHEN C H. Effect of synthesis conditions on electrochemical properties of $LiNi_{1-y}Co_yO_2$ cathode for lithium rechargeable batteries [J]. Journal of Power Sources, 2002, 114: 244−252.

[16] WANG G X, ZHONG S, BRADHURST D H, DOU S X, LIU H K. Synthesis and characterization of $LiNiO_2$ compounds as cathodes for

rechargeable lithium batteries [J]. Journal of Power Sources, 1998, 76: 141−146.

[17] LI W, REIMERS J N, DAHN J R. In situ X-ray diffraction and electrochemical studies of $Li_{1-x}NiO_2$ [J]. Solid State Ionics, 1993, 67(1−2): 123−130.

[18] OHZUKU T, UEDE A, NAGAYAMA M. Electrochemistry and structural chemistry of $LiNiO_2$ (R3-m) for 4 volt secondary lithium cells [J]. Journal of the Electrochemical Society, 1993, 140(7): 1862−1870.

[19] MOSHTEV R, ZLATILOVA P, VASILEV S, BAKALOVA I, KOZAWA A. Synthesis, XRD characterization and electrochemical performance of over lithiated $LiNiO_2$ [J]. Journal of Power Sources, 1999, 81−82: 434−441.

[20] ALCANTARA R, LAVELA P, TIRADO J L, STOYANOVA R, ZHECHEVA E. Changes in structure and cathode performance with composition and preparation temperature of lithium cobalt nickel oxide [J]. Journal of the Electrochemical Society, 1998, 145(3): 730−736.

[21] COVER R K B, KANNO R, MITCHELL B J, YONEMURA M, KAWAMOTO Y. Effects of sintering temperature on the structure of the layered phase $Li_x(Ni_{0.8}Co_{0.2})O_2$ [J]. Journal of the Electrochemical Society, 2000, 147(11): 4045−4051.

烧结温度对 $LiNi_{0.8}Co_{0.1}Mn_{0.1}O_2$ 材料倍率性能和循环性能的影响

李向群[1]，熊训辉[2]，王志兴[2]，陈启元[1]

1. 中南大学 化学化工学院，长沙 410083；
2. 中南大学 冶金与环境学院，长沙 410083

摘　要：以共沉淀法制备的球形 $Ni_{0.8}Co_{0.1}Mn_{0.1}(OH)_2$ 和 $LiOH·H_2O$ 为原料，研究烧结温度对 $LiNi_{0.8}Co_{0.1}Mn_{0.1}O_2$ 材料形貌、结构以及材料循环性能和倍率性能的影响。SEM 和 XRD 结果表明：温度对材料形貌和结构有较大的影响，控制适当温度既能保证材料具有良好的形貌，也能抑制材料中锂镍的混排。电化学测试结果显示，当烧结温度从 700 °C 升高至 750 °C 时，材料性能逐渐提高，但是温度过高会恶化材料的性能。750 °C 和 780 °C 烧结材料的循环性能几乎一致，200 次循环后容量保持率为 71.9%，但 780 °C 烧结材料的倍率性能低于 750 °C 材料的，其原因归结于温度过高，锂镍的混排加剧。在小电流充放电时，对材料性能影响有限，但是在大电流充放电时，3*a* 位的 Ni^{2+}将严重阻碍锂离子的扩散。

关键词：锂离子电池；$LiNi_{0.8}Co_{0.1}Mn_{0.1}O_2$；煅烧温度；循环性能；倍率性能

(Edited by Hua YANG)